

Investigating the Large Asperity of the 1999 Chichi, Taiwan Earthquake

James MORI, Hidemi TANAKA*, and Kuo-Fong MA**

* Faculty of Science, University of Tokyo, Japan

** Geophysical Institute, National Central University, Taiwan

Synopsis

We use seismic data and borehole temperature data to infer characteristics of the faulting process of the 1999 Chichi, Taiwan earthquake. Inversion of strong-motion data and associated observations of surface faulting show that the northern portion of the Chelungpu fault had very large displacements in excess of 10 m, while the southern part of the fault had much smaller displacements of 1-2 m. In contrast the levels of accelerations and damage show a very different pattern, with much more severe high frequency ground motions in the south and extensive damage to small buildings. In the north the levels of acceleration and associated damage are relatively low, considering the very large fault displacements. These differences in observed ground motions are attributed to differences in dynamic fault behavior during the earthquake. Determinations of radiated seismic energy and estimates of frictional heat produced by the earthquake are used to put together the energy budget for the earthquake. We obtained a total radiated energy of 1.1×10^{16} J and frictional heat of 2×10^{17} J. These values give a seismic efficiency of about 5%. We also looked at the energy balance separately for the northern and southern portions of the Chelungpu fault. The northern part produced much lower heat, even though the slip was much larger, implying a lower value of friction. Also, the northern part produced more radiated seismic energy, so the seismic efficiency for the north is higher than for the south. The low values of friction for the northern portion, provide a good explanation for the low levels of high frequency radiation and the lower levels of damage in the nearby areas.

Keywords: Chichi, Taiwan earthquake, frictional heat, radiated energy, temperature

1. Introduction

The September 21, 1999 Chichi, Taiwan earthquake (Mw 7.6) is notable for the large surface fault displacements (up to 8 m) that were observed along the northern portion of the Chelungpu fault (Ma et al., 1999). One of the most interesting observations from the earthquake is that the areas close to the portions of the fault that had the largest displacements, had relatively low acceleration levels and relatively low levels of damage to small (1-3 stories) buildings (Ma et al., 1999). The strong motion data recorded near the fault in the north show very large ground velocities, indicating that the fault

slip velocity was very fast, but the relatively low levels of high frequency indicate a very 'smooth' rupture (Ma et al., 2003). An example of the lack of damage close to the fault are shown in Fig 1. In contrast, the regions close to the fault in the south, where the surface fault displacements were much smaller (1-2m), had higher levels of accelerations and more severe damage to small buildings (Fig. 2). Since the earthquake was very well recorded on the dense array of strong-motion instruments that was installed in Taiwan (Liu et al., 1999), the recorded seismic data provides a good opportunity to study the characteristics of the faulting process and compare

the differences between portions of the fault that had very large slip and relatively small slip. In addition, boreholes were drilled on the northern and southern portions of the fault, which yielded samples of the faulting surface and temperature profiles with depths. The combination of seismic and temperature data provides some new insights into the characteristics of the fault, especially the frictional and stress levels associated with the earthquake.



Fig. 1. Undamaged brick wall near northern portion of the Chelungpu fault. Person in far right background is standing on the fault.



Fig. 2. Collapsed first story of building in ChungLiao Town, near southern portion of the Chelungpu fault, where 95% of the buildings were severely damaged.

2. Large Asperity

There have been numerous source inversions of the Chichi earthquake using teleseismic data, strong-motion data, Global Positioning System (GPS) data, and combinations of these data sets (e.g. Kikuchi et al., 2000, Ma et al., 2000, Ma et al., 2001, Wue et al.,

2001, Zeng and Chen, 2001, Oglesby and Day, 2001, Chi et al., 2001, Ji et al., 2001, Yoshioka, 2001). One common feature of all the source models is the large area of slip in the north, which has displacements of 10-20 meters, depending on the specific models. Fig. 3, shows the slip distribution from a model by Ma et al., 2001, which clearly shows the large area of slip in the north. This area of large slip is largely recognized as an ‘asperity’ or region of large slip on the fault plane. The locations and sizes of ‘asperities’ have recently been the focus of numerous studies, since they may control the faulting process in the large earthquakes and also control the distribution of strong ground motions in calculated simulations (e.g. Irikura, 1986).

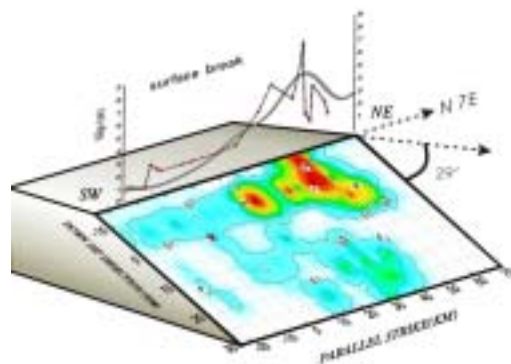


Fig. 3. Slip distribution model from Ma et al., 2001 showing the large amounts of slip on the northern portions of the fault.

3. Radiated Energy Estimate

We estimated the radiated energy for the earthquake following Kanamori et al., (1993) using the regional strong motion records. We used 63 records that had good azimuthal coverage around the fault. We did not use the records that were very close to that fault, since they are dominated by near-field terms from portions of the fault close to the recording station, and do not accurately represent the radiated energy for the whole earthquake. We obtained an average value of 1.1×10^{16} J for the radiated energy. This value is also consistent with the values obtained

from for teleseismic recordings (0.88×10^{16} J) by Venkataraman (2002)

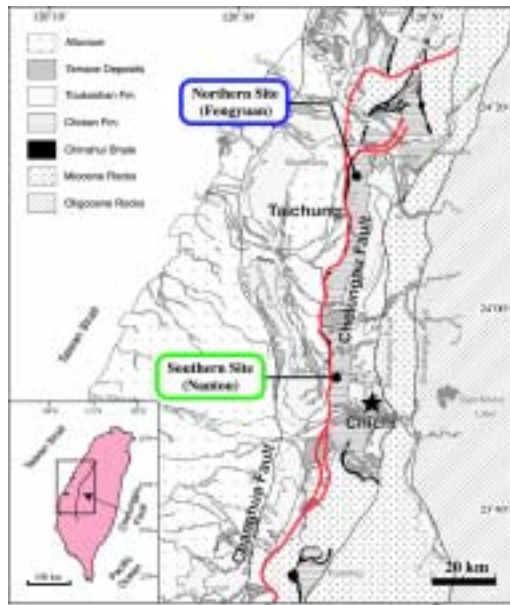


Fig. 4. Map of surface rupture of the Chelungpu fault and locations of the two borehole sites.

4. Temperature Profiles in Boreholes

Two boreholes were drilled into the northern and southern portions of the Chelungpu fault during December 2000 to January 2001, 15 to 16 months following the earthquake. The locations of the boreholes is shown in Fig. 4. The northern borehole penetrated the fault at a depth of about 325 m, and the southern borehole penetrated the fault at about 175 m. Following the drilling, the temperature was measured in the borehole using a downhole fiber thermometer. The temperature profiles at depths close to the fault are shown in Fig. 5. Note that there is a slight rise in temperature in both boreholes where the temperature profiles cross the fault. In the north the temperature anomaly is about 0.1 C° , and in the south about 0.4 C° .

Since both boreholes show a temperature change close to the fault, we interpret this temperature increase as due to faulting during the earthquake. A simple explanation is that the temperature increase is due to frictional heating. Very little is known about

the frictional heat due to faulting, but simple calculation show that the temperature rise at the time of the time of the earthquake could be on the order of 100 to 1000 C° , depending on the stress levels and thickness of the fault zone (Kanamori and Heaton, 2002).

The higher temperatures on the southern part of the fault, are also consistent with the observations of pseudotachylites that were found in the fault zone for the core sample in the south.

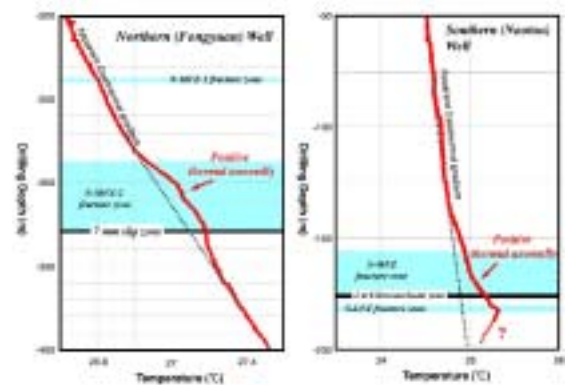


Fig. 5. Temperature profiles in northern and southern boreholes. Note that there is a slight increase of temperatures in both profiles in the region of the fault.

5. Estimates of Frictional Heat

Using the simple model of Lachenbruch and Sass (1980) frictional heat produced by a fault, we tried to model the temperature anomaly observed across the fault. We assumed the physical constants shown in Table 1 and then found values of the coefficient of friction and heat diffusivity that best fit the data.

Table 1. Constants used to model borehole temperature profiles

	North	South
Time t (s):	4.36×10^7	4.36×10^7
Normal stress (MPa)	6.44	4.64
Displacement (m):	4.0	1.0
Density (kg/m^3):	2600	2600
Specific heat ($\text{J}/\text{kg} \cdot \text{K}$):	1140	1140
Heat conductivity ($\text{W}/\text{m} \cdot \text{K}$):	1.5	1.5

For the north the slip was large but the temperature change was relatively small. This results in a low coefficient of friction of 0.1 to 0.2. In the south, the larger temperature change associated with a smaller fault displacement gave a larger value of 0.9 to 1.0 for the coefficient of friction. The heat diffusivity, which is controlled by the width of the temperature anomaly, was estimated to be $2.0 \times 10^6 \text{ m}^2/\text{sec}$ and $5.0 \times 10^7 \text{ m}^2/\text{sec}$ for the north and south, respectively. Fig. 6, shows the modeling of the temperature using these parameters along with the observed data.

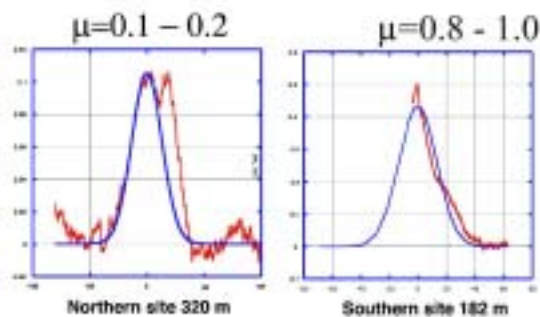


Fig. 6. Modeling of temperature profiles in the northern and southern boreholes.

An interesting result is the difference in the coefficient of friction between the different portions of the fault. If these results are correct, they indicate different dynamic friction levels for the large asperity as compared to the rest of the fault. Using these values for the coefficient of friction, we can estimate the total heat production for the earthquake, assuming that the normal stress is equal to the lithostatic pressure. For the large slip in the north, we assume an area of $20 \times 30 \text{ km}^2$ and with a coefficient of friction of 0.2, we obtain a heat production of $3.2 \times 10^{16} \text{ J}$. For the rest of the fault, we use an area of $60 \times 30 \text{ km}^2$ and a coefficient of friction of 0.8 to obtain a value of $1.7 \times 10^{17} \text{ J}$. The sum of these two values gives a total frictional heat of $2.0 \times 10^{17} \text{ J}$.

There are several major uncertainties in this analysis, one of which is whether or not the temperature measurements from relatively shallow depths are representative of the seismic faulting. It is hard to evaluate this problem, however, the similar temperature signatures across the fault for both the north and south boreholes suggest that we are observing real temperature changes associated with the faulting. Another problem, is that in this simple analysis, we assume all the heat is redistributed by conduction. The presence of fluids can significantly alter this process, and further work needs to be done to account for this possibility.

6. Discussion

Using the values of radiated energy and frictional heat, estimated in the previous sections, we show the energy balance of the earthquake in Fig. 7. This figure shows the stress level on the fault, as a function of slip**fault area*. This type of figure is commonly used to show the stress levels before, during, and after an earthquakes (e.g Lachenbruch and Sass, 1980). The upper triangle shows the amount of total radiated energy and the lower rectangle shows the amount of frictional heat. In this simple interpretation, we assume that the fracture energy is relatively small. If the rupture energy is close to the shear velocity, as observed in most of the source models, the fracture energy is small (Kanamori and Heaton, 2002).

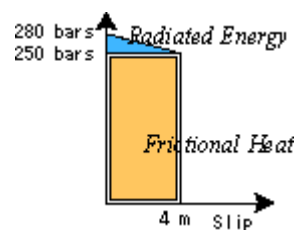


Fig. 7. Total energy budget for the earthquake

Adding the two types of energy, gives an estimate of the absolute stress level prior to the earthquake. For this stress level, we obtain an average value of

about 25 to 30 MPa. The ratio of the radiated energy to the total energy gives an estimate of the seismic efficiency. The average seismic efficiency we obtain is 5%. Estimates of stress level and seismic efficiency for large earthquakes are generally difficult to obtain, since there are very few measurements of the heat generated by large earthquakes. The values presented here are some of the first observational values for these parameters from large earthquakes.

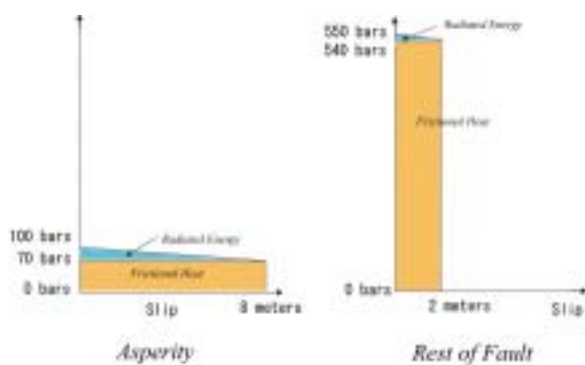


Fig. 8. Energy budgets for the northern (asperity) and southern portions of the fault.

The northern and southern portions of the fault appear to have ruptured differently during the earthquake. The large displacements and velocities of the fault in the north imply a large amount of radiated energy. Looking at teleseismic records, the large asperity in the north accounts for about 70% of the total radiated energy. The estimates of heat and coefficient of friction are much smaller in the north. Combining these observations of radiated energy and frictional energy, we obtain the total energy budget for the north, as shown in Fig. 8. The large radiated energy and smaller frictional heat gives a smaller value of absolute stress and seismic energy compared to the average for the whole earthquake (Fig. 7). In the south, the radiated energy is relatively low and the frictional heat is high, which results in high levels of stress and seismic efficiency (Fig. 8).

The low level of friction in the north may give an explanation for the low levels of acceleration and damage. It has been proposed that the reduction of

dynamic friction for the large slip in the north may have been caused by fault lubrication (Ma et al, 2003) or other mechanisms such as fault melting or fluid pressurization.

7. Conclusions

From strong motion records and borehole temperature measurements, we obtain estimates of the stress levels and total energy budget for the 1999 Chichi, Taiwan earthquake. These are some of the first observational values of these parameters for a large earthquake. For the whole earthquake, we obtain a radiated energy of 1.1×10^{16} J. and frictional heat generation of 2.0×10^{17} J. Combining these values gives a seismic efficiency of 5% and an absolute level of stress prior to the earthquake of about 28 to 30 MPa.

The large portion of fault that had very large slip in the north appears to have behaved very differently from the portion that had smaller slips in the south. The northern portion seems to have generated less heat, even though the slip was larger. This implies a lower level of dynamic friction. The coefficients of friction for the north and south are estimated to be 0.1 to 0.2 and 0.7 to 1.0, respectively. The seismic efficiency in the north and south is estimated to be 1% and 15%, respectively. The lower level of dynamic friction may provide an explanation for the smooth slip in the north that produced relatively low levels of acceleration and relatively less damage to small buildings.

References

- Chi, W.-C., Dreger, D., A. Kaverina, A. (2001): Finite source modeling of the 1999 Taiwan (Chi-Chi) earthquake derived from a dense strong-motion network, *Bull. Seismol. Soc. Am.*, Vol. 91, pp. 1144-1157.

- Irikura, K. (1986): Prediction of strong acceleration motion using empirical Green's functions, Proc. 7th Japan Earthquake Eng. Symp., pp. 151-156.
- Ji, C., Helmberger, D.V., Song, T.R., Ma, K.-F., and Wald, D.J. (2001): Slip distribution and tectonic implication of the 1999 Chi-Chi, Taiwan, earthquake, Geophys. Res. Lett. 28, pp. 4379-4382.
- Kanamori, H. and Heaton, T.H. (2002): Microscopic and macroscopic physics of earthquakes, in Geocomplexity and the Physics of Earthquakes, J. Rundle, D. L. Turcotte, W. Klein, Eds., Geophysical monograph no. 120, American Geophysical Union, Washington D.C., 147p.
- Kanamori, H., Mori, J., Hauksson, E., Heaton, T.H., Hutton, L.K., Jones, L.M. (1993): Determination of earthquake energy release and M_L using Terrascope, Bull. Seismol. Soc. Am., Vol. 83, pp. 330-346.
- Kikuchi, M., Yagi, Y., and Yamanaka, Y. (2000): Source process of the Chi-Chi, Taiwan earthquake of September 21, 1999 inferred from teleseismic body waves, Bull. Earthquake Res. Inst. Univ. Tokyo, Vol. 75, pp.1-14
- Lachenbruch, A.H. and Sass, J.H. (1980): Heat flow and energetics of the San Andreas fault zone, J. Geophys. Res., Vol. 85, pp 6185-6222.
- Liu, K.-S., T.-C. Shin, T.-C., and Tsai, Y.-B. (1999): A free-field strong motion network in Taiwan: TSMIP, Tao, Vol. 10, pp. 337-396.
- Ma, K-F., Brodsky, E., Kanamori, H., Mori, J., and Song, A. (2003): Evidence for Fault Lubrication during the 1999 Chi-Chi, Taiwan, Earthquake (Mw7.6). Geophys. Res. Lett., Vol. 30, 10.1029/2002GL015380.
- Ma, K.-F., Lee, C.-T., Tsai, Y.-B., Shin, T.-C., and Mori, J. (1999): The Chi-Chi, Taiwan earthquake; Large surface displacements on an inland thrust fault, EOS Trans. Am. Geophys. Union, Vol. 80, pp. 605 and 611.
- Ma., K-F., Mori, J., Lee, S.J., Yu, S.B. (2001): Spatial and temporal distribution of slip for the 1999 Chi-chi, Taiwan earthquake, Bull. Seismol. Soc. Am., Vol. 91, pp. 1069-1087.
- Ma., K-F., Song, T.R., Lee, S.J., Wu, S.I. (2000): Spatial slip distribution of the September 20, 1999, Chi-Chi Taiwan earthquake inverted from teleseismic data, Geophys. Res. Lett., Vol. 27, pp. 3417-3420.
- Oglesby, D. D. and Day, S.M. (2001): Fault geometry and the dynamics of the 1999 Chi-Chi (Taiwan) earthquake, Bull. Seismol. Soc. Am., Vol. 91, pp. 1099-1111.
- Venkataraman, A. (2002): Investigating the mechanics of earthquakes using macroscopic seismic parameters, PhD Thesis, California Inst. Technology, 169 p.
- Wu, C., Takeo, M., Ide, S. (2001): Source process of the Chi-Chi Earthquake: Joint inversions of strong motion data and global positioning system data with a multifault model, Bull. Seismol. Soc. Am., Vol. 91, pp. 1128-1143.
- Yoshioka, S. (2001): Fault slip inverted from surface displacements during the 1999 Chi-Chi, Taiwan earthquake, Bull. Seismol. Soc. Am., Vol. 91, pp. 1182-1189.
- Zeng, Y. and Chen, C.-H. (2001): Fault rupture process of the 20 September 1999 Chi-Chi Taiwan, earthquake, Bull. Seismol. Soc. Am., Vol. 91, pp. 1088-1098.

集集台湾地震のアスペリティの破壊過程の調査

Investigating the Large Asperity of the 1999 Chichi, Taiwan Earthquake

James MORI · 田中秀実 · Kuo-Fong MA

京都大学防災研究所地震予知研究センター
東京大学理学部地学科固体地球講座
中央大学地球物理研究所

要旨

地震のデータとボアホール温度のデータを使って、1999年台湾集集地震のすべりのプロセスの性格を推定した。車籠埔断層の北部では10メートルを超える大きなずれが見られた一方、南部のずれは1～2メートルとはるかに小さかった。ところが意外にも、加速度と被害は全くちがったパターンを示し、南部では激しい高周期の地面の揺れと小さな建造物への大被害が見られた。その一方、北部では加速度のレベルが比較的 low、それに伴う被害も、断層のずれの大きさから考えると軽かった。この違いは地震の際の断層の動き方の違いに帰せられる。地震の放射エネルギーと、発せられた摩擦熱を計算すれば、総エネルギーがどのように配分されたか知ることができる。この地震では、放射エネルギーは 1.1×10^{16} J、摩擦熱は 2×10^{17} J という値を得た。従って地震効率は約5%ということになる。さらに、車籠埔断層の北部と南部のそれぞれについて、こうしたエネルギー・バランスを計算した。この結果、北部ははるかに大きいすべりがあったにもかかわらず熱量は低く、摩擦の値の低かったことを示している。また、放射エネルギーは北部の方が大きく、地震効率は南部より高い。北部の摩擦の値の低さは、高周波のレベルが低いことや周辺地域の被害が比較的軽かったことの説明になっている。

キーワード：集集台湾地震、摩擦熱、放射エネルギー、温度